Status of the LHCb experiment

CERN-RRB-2017-034

26 April 2017

1 Introduction

All components of LHCb functioned well throughout the 2016 run, and the experiment was able to respond effectively to the very high efficiency of machine operation. A data set corresponding to $1.7\,\mathrm{fb}^{-1}$ at $13\,\mathrm{TeV}$ was collected in pp collisions, more than doubling the experiment's sample size in many key physics channels. The detector also collected a larger than anticipated sample of data in pPb collisions at the end of the year, and in fixed-target mode, using LHCb's unique SMOG gas-injection system. No major interventions have been required during the End of Year Technical Stop, and the detector is ready for the resumption of data taking. In parallel, modifications have been implemented in the operations strategy that should lead to corresponding improvements in data taking and processing in 2017. More information can be found in Secs. 2 and 3.

The year 2016 was highly successful for LHCb physics output, with 64 papers submitted to journals. This total is more than achieved in any previous year when the collider has been operating. In total 370 papers have now been published or submitted. Highlights since the last RRB include the observation of five new excited Ω_c^0 states [1], the release of the first results from the SMOG fixed-target data taking [2,3], and the first single-experiment observation of the ultra-rare decay $B_s^0 \to \mu^+\mu^-$ [4]. These results are discussed in Sect. 4.

Finally, significant efforts have been invested into preparations for the LHCb Upgrade, scheduled to be installed in Long Shutdown 2. This work is described in a separate document [5].

2 Detector sub-systems

After a very successful operation of the LHCb detector in 2016, the Extended Year End Technical Stop (EYETS) was dedicated to maintenance and consolidation work at Point 8. This included major interventions on the two overhead cranes and on the personnel lift. These interventions had to be planned with great attention to avoid any interference with the work planned on the detector and its services. Almost all consolidation activities have been successfully completed and only very few tasks remain, which are schedule for the end of the EYETS. Currently, the preparation for a smooth restart of Run 2 is in full swing and the re-commissioning of the experiment will follow right after.

2.1 Vertex Locator (VELO)

The VELO continued to take high quality data throughout Run 2. The detector ageing was continuously monitored via regular IV (current vs. voltage) scans and dedicated CCE (charge collection efficiency) scans. Moreover, the so-called "alert" system provides an uninterrupted record of leakage currents during regular operation and reacts in case of unforeseen changes.

The detector monitoring has evolved during the year. The old GUI had become unmaintainable and was replaced with a dual system. This comprises an offline GUI, which allows expert operations and an easy plot generation on the LHCb cluster, and a web-based GUI for read-only operations, which is accessible from anywhere with a CERN login and allows easy access for out of control-room checks. Both GUIs have a very similar structure and are based on the same configuration file. In 2017, the monitoring will be complemented with the addition of more flexible long-term trending.

The leakage currents in the VELO continue to evolve, as shown in Fig. 1, and following the CCE scan analysis, voltages will need to be raised during the 2017 run. The strategy was adopted of running the IV scans to a higher voltage than the operation voltage in order to train the sensors and avoid tripping during operation. In addition, there have been two interventions on the HV system, and a further maintenance is planned before the start of 2017 data taking. The main goal is to remove inconsistencies which have been found in the code among different channels and to perform a controlled run of the sensors at an increased voltage, in preparation for the physics run.

Towards the end of last year's data taking some anomalies were seen in the pump that services the tertiary CO_2 cooling loop for the right half of the detector, which from time to time suffered drops in pressure. The decision was taken to postpone any intervention until the end of data taking and to monitor the situation closely. The detector was vented on December 7th and has been kept under neon up to now. The planned intervention on the faulty pump was carried out on January 31st, using the backup pumps to minimise any impact on the detector. The worn elements were replaced and the pump has operated stably since then. The opportunity was taken to inspect the cooling system for the impact of the maintenance activities which had taken place during 2016. The additional isolation and dry air circulating system was shown to be very successful: the regions where ice had previously accumulated were observed to be completely dry.

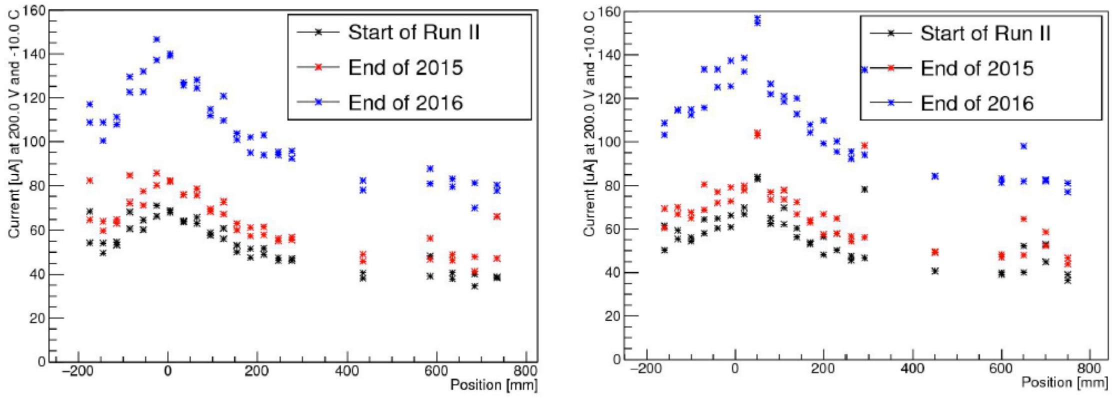

Figure 1: Monitored currents as a function of z position in the VELO, showing the evolution through 2015-2016 for sides A (left) and C (right).

2.2 Silicon Tracker (ST)

The Tracker Turicensis (TT) and Inner Tracker (IT), which together form the Silicon Tracker (ST), ran successfully throughout 2016. Both sub-detectors are operated by the central LHCb shift crew, with support from an on-call piquet and a small team of experts. The fraction of working channels is currently 99.68% and 98.96% in the TT and IT, respectively. During the EYETS, one major intervention was performed on three TT modules, while no work was required on the IT stations. The detector was left in a safe state during the EYETS with no power on the front-ends and no high voltage applied to the sensors. The sensors are cooled at all times except for short periods during standard maintenance of the cooling plants.

Three TT modules with a relatively high number of low noise channels were repaired in January. The modules were removed and the damaged read-out hybrids were replaced. The most problematic module had a total of 152 channels masked before repair, resulting in a hit efficiency of $< 70\%$, while now it only has four low-noise channels. In total, 232 channels were recovered, amounting to 0.16% of the detector. This problem was first observed in some modules shortly after installation, and was traced to broken bond wires between the pitch adapter and the innermost bond row of the read-out chip. New hybrids were produced with an increased distance between the pitch adapter and the read-out chip. The three modules that were removed this year had bonds that were broken on the read-out chip side, and not, as previously expected, on the pitch adapter side. Two of the modules already had new hybrids after repairs in 2010/11, indicating that an increasing distance between the pitch adapter and the read-out chip had not solved the issue.

After the re-installation of the TT modules, it was intended to leave the detector in a warm state as there was no monitoring of the temperature and humidity in the detector box, due to an intervention on the cooling of the detector electronics. However, after this intervention was completed and the electronics were recovered, it was discovered that the detector had already been cooled to zero degrees. The cause of this potentially serious incident is still under investigation.

There were a few other minor problems in 2016. Three broken VCSEL diodes (all in TT) were replaced during technical stops. In addition, the three HV CAEN boards that developed faults in single channels (reported in the previous RRB document) have now been repaired. All WinCC-OA projects were upgraded during the EYETS; both sub-systems have been tested and some minor issues were fixed.

A Brandeis CCD Angle Monitor (BCAM) system has been used to monitor the movement of the IT stations. The system measured movements of $(x, y, z) \sim (0.3, 0.4, 10)$ mm between magnet-on and magnet-off periods for the station closest to the magnet; stations further away have less pronounced movements. A smaller effect of $\approx 30\,\mu$m was seen when powering on/off the electronics. The overall scale of movement of the stations is consistent between 2015 and 2016. Comparison of the BCAM measurements with data from the track-based online alignment system is ongoing, and the aim is to use the BCAM measurements to predict more reliably when an update of the alignment constants is needed.

Radiation damage of the silicon sensors is monitored using two methods: measurements of the depletion voltage obtained from periodic CCE scans, and leakage current measurements taken continuously throughout the year. In both cases, the analysed data are consistent with predictions from simulation, and the detector is ageing as expected.

2.3 Outer Tracker (OT)

The various Outer Tracker hardware components in the LV, HV and readout chains operated very reliably, and no repairs were needed during the last few months of running in 2016, nor during the EYETS.

The Outer Tracker participated in the successful proton-lead data taking at the end of 2016, following on from the experience gained during the lead-lead run at the end of the preceding year. Studies have continued for both samples. Due to the relatively large straw diameter of 5 mm, the event occupancies during the Pb-Pb run reached values all the way up to 100% for the collisions at highest centrality. Nevertheless, interesting physics results are anticipated for Pb-Pb collisions with value of the centrality up to 40%. The event occupancies for p-Pb running, shown in Fig. 2, were modest and did not require any special treatment.

The various hardware components in the LV, HV and readout chains operated very reliably, and no repairs were needed during the last few months of running in 2016, nor during the EYETS.

In the upcoming 2017 running period, the reported desynchronisations of individual "control boxes" (which each serve 4% of the OT) will be closely watched, and when needed the optical fibre carrying the clock signal will be cleaned to improve the signal.

In addition, the OT occupancy will be reduced by implementing an extra cut at the lowest trigger level, which will reject events which are preceded by a busy

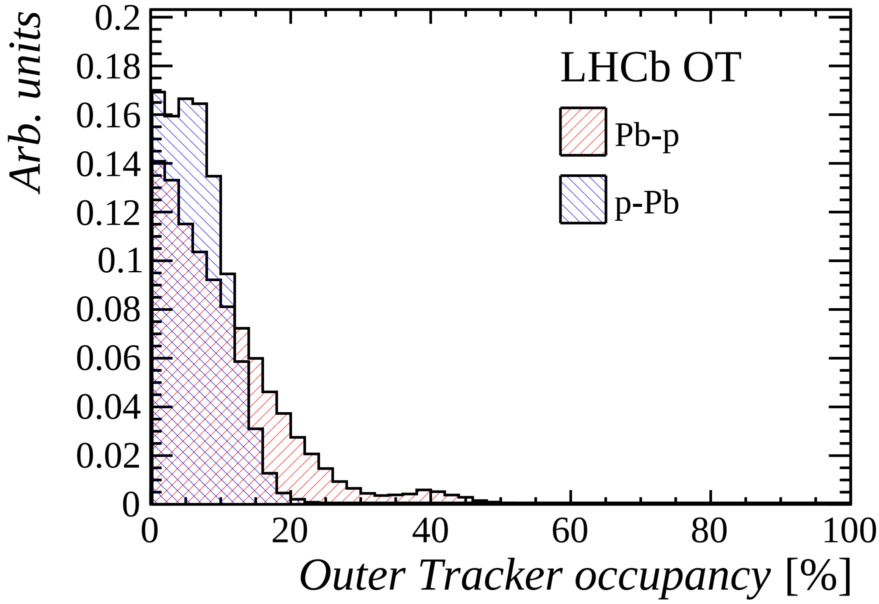

Figure 2: OT occupancy during the 2015 proton-lead run. The two distributions correspond to the data taken with the different directions of proton beam.

bunch crossing. This selection will reduce the fraction of spill-over hits in the OT, and as such reduce the total OT data volume, which is currently the bottleneck in the LHCb data rate. At the same time, this cut will result in cleaner events, facilitating the event reconstruction.

2.4 RICH system

The RICH detectors performed very well in 2016, which was mainly a year of routine operation with some hardware issues that are being addressed during the EYETS. On the software side, everything functioned as expected. New developments on alignment and calibration are expected before the start of data taking in June 2017.

Figure 3 shows a comparison of the particle identification performance between Run 1 and Run 2 in terms of kaon identification and pion mis-identification efficiencies. Due to the change in the beam energy, events are re-weighted by the number of tracks in the event and the performance is presented in bins of momentum and pseudorapidity. The removal of the aerogel allows for more photons from the gas radiator to reach the photon detectors and therefore the performance at low momenta has improved significantly.

Some intermittent problems were observed in the electronics of two rather central HPDs in RICH1. As the origin of the problem was not clear and the

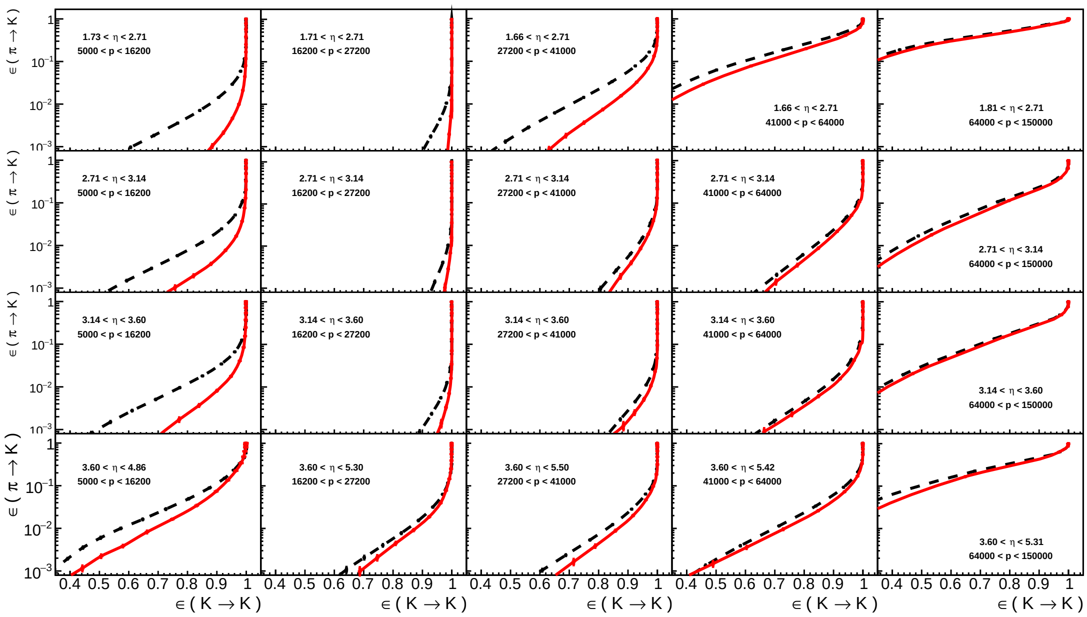

Figure 3: Performance comparison of kaon identification and pion mis-identification efficiencies in Run 1 (black dashed lines) and Run 2 (red lines) in bins of momentum and pseudorapidity. The performance at low momentum is significantly better in Run 2.

possibility of future failure existed, the RICH1 lower box was extracted for repairs. A number of electronic components were exchanged and two HPD columns were swapped as a risk mitigation strategy. Given that the box was accessible, six HPDs with higher ion feedback were replaced as well. HPDs are also being replaced in RICH2 as part of the annual maintenance. The total number of HPDs that need reprocessing before the end of Run 2 is being estimated. There was no need to install new UKL1 boards; however, a prototype board exists as well as the infrastructure to install more boards, if necessary. It takes only a matter of weeks to manufacture new boards in case the need arises, or a problem arises with the number of available spare boards.

2.5 Calorimeters (SPD, PS, ECAL and HCAL)

The maintenance of the calorimeter system is finished and the detectors are ready for 2017 data taking. During the EYETS one malfunctioning VFE board in the PS and the 58 most degraded HCAL PMTs were replaced with spare tubes. In addition, a few unstable and malfunctioning ECAL and HCAL components (PMT Cockcroft-Walton HV sources and LED drivers) were fixed. Figure 4 illustrates the resulting ECAL and HCAL cell performance using data from the LED monitoring systems. As shown in the figure, all cells are currently operational.

The performance of the ECAL π^0-based online calibration has been considerably improved. Firstly, the algorithm used to write calibration DSTs was modified

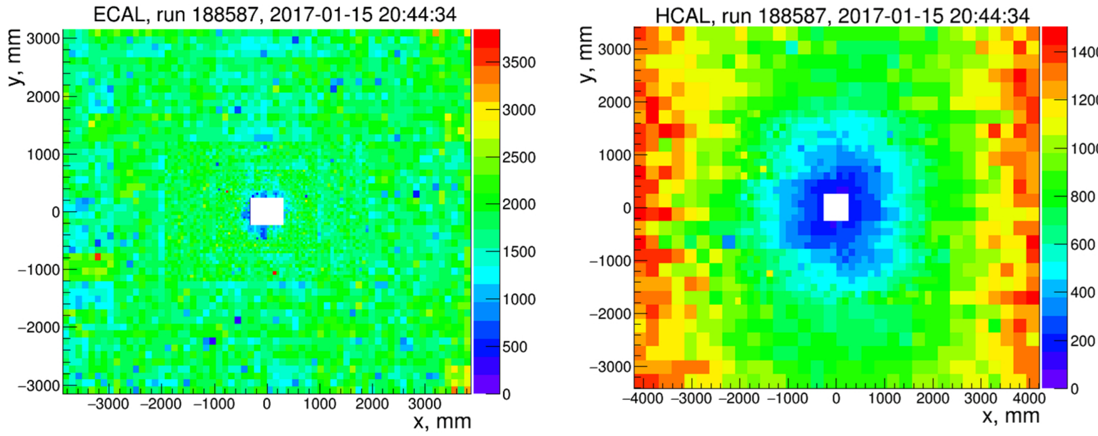

Figure 4: Scan of the ECAL (left) and HCAL (right) cells using the LED system: all cells are operational.

as to include cell energy depositions from a larger area around the cluster seed than the 3x3 cells that had been included in the past; this approximation was in fact the source of a $\sim$1% discrepancy between the π^0-based online calibration and the offline reconstruction. In addition, the procedure used to fit the π^0 mass distributions was revised, resulting in a very significant gain in speed: one to two minutes per iteration compared to $\sim$20 minutes before. Finally, the production of the femto-DSTs was optimised by creating them directly from the raw data files without passing through the full DST files. The calibration procedure will be applied once per month during the 2017 run.

2.6 Muon system

In 2016, the muon chambers operated in a very stable manner with efficiencies per station exceeding 98%. During the initial part of the run, the LHC luminosity ramp produced a larger than usual number of HV trips in the MWPCs. All affected channels were trained with beam at nominal HV, which in most cases allowed the normal current value of $\sim$140 nA to be recovered after a few days of operation (see Fig. 5). In the second part of the run, the rate of HV trips went back to the normal level of one per week.

During the EYETS, a single missing chamber in M1, from a total of 1380 chambers for the whole muon system, was recovered by replacing a broken channel in one of the service boards which controls the front-end electronics. In addition, $\sim$50 non-operating or noisy channels were identified from a total of 26k FEE channels. Given that none of these faults is expected to have a significant impact on the physics performance, it was decided not to open the detector walls to fix them.

Another important activity carried out during the EYETS was the training of the MWPC chambers under negative HV polarity, which is a proven technique for

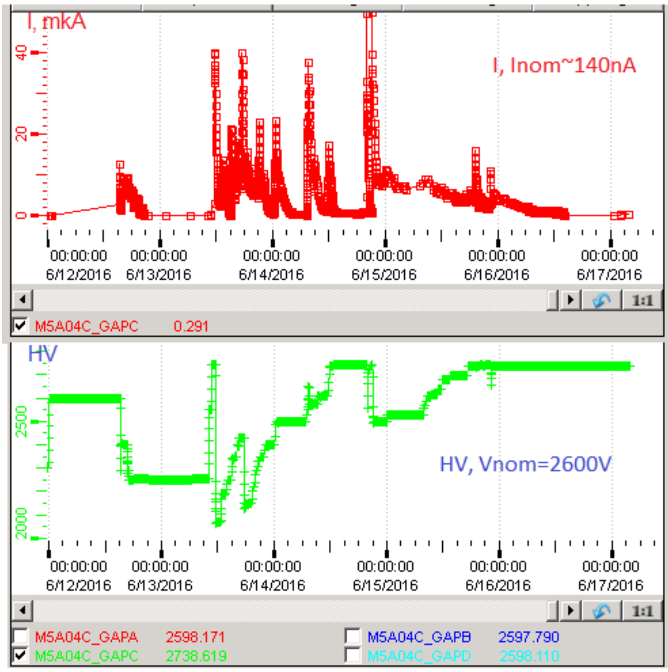

Figure 5: Current, in μA, drawn by an M5 chamber gap during five days of operation with and without beam (top) and the corresponding HV setting (bottom).

removing Malter currents and other deposits on the cathode planes. Around 150 chambers, corresponding to 600 gaps, were successfully treated with this procedure. The training consisted of applying a negative voltage to the anode wires, with values slowly decreasing down to -2.3 kV, achieving a dark current lower than $\sim$50 nA. Following this training the channels were tested again at positive polarity to match the quality criterion of having a dark current of $\sim$10 nA at +2.85 kV.

In the 2017 run, first collisions will be used to check and finely adjust the muon system timing and spatial alignment.

2.7 Forward shower counters, HeRSCheL

The HeRSCheL detector continued to collect data throughout the remainder of the 2016 running period, including during heavy ion operation. Throughout 2015 and 2016 the reduction in the light yield of the scintillators was closely monitored. Significant degradation was observed, as shown during 2015 alone for one station in Fig. 6. During data-taking this was compensated at regular intervals by adjusting the high voltage applied to the photomultipliers to ensure that a typical average signal from the detector was maintained.

At the end of 2016 data taking, the counters were unmounted and moved from the tunnel to the surface. During the EYETS replacement scintillators and light-guides were prepared for all twenty counters, ready to replace the irradiated components. Measurements have been made using cosmic rays in order to gain an understanding of the degradation of the detector, including studies of the photomultipliers, overall scintillator light yield and, since the corner closest to the beam is only a few centimetres away, non-uniform scintillator irradiation. Following replacement of the light-guides and scintillators, the new modules are also currently being studied using cosmic rays in order to characterise the signal obtained from each counter, depending on the applied high voltage, ready for 2017 data-taking.

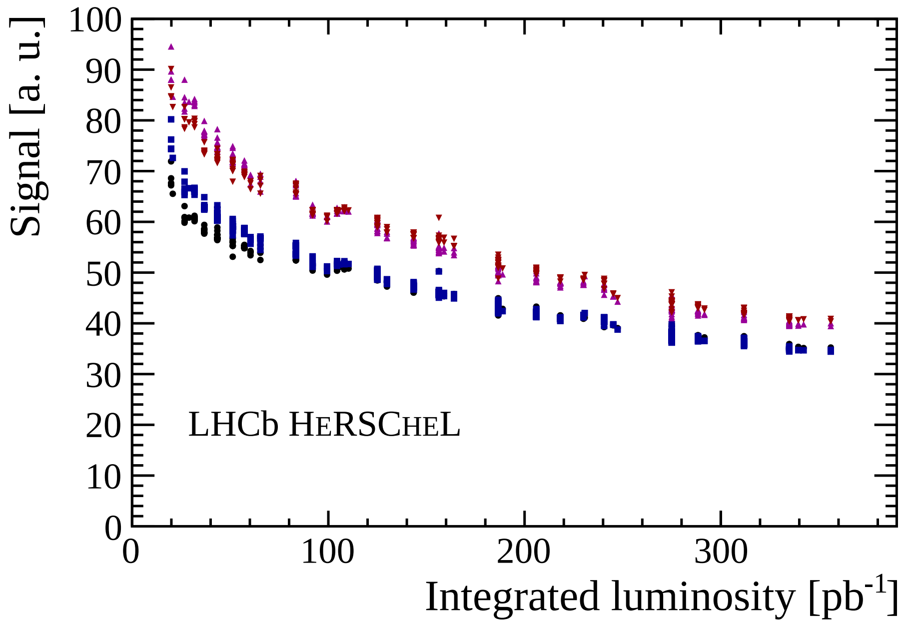

Figure 6: Relative variation in scintillator light yield during the 2015 data-taking, for one of the HeRSCheL detector stations. The four sets of points correspond to the four quadrants of scintillator mounted at that point in the LHC tunnel.

The use of HeRSCheL information in the LHCb hardware trigger remains a high priority, as it is hoped that this will lead to significantly higher trigger efficiency for Central Exclusive Production of certain hadronic states. Progress has continued during the EYETS in developing the firmware and software required to operate HeRSCheL as part of the L0 trigger. New firmware for the existing read-out board has been prepared and tested successfully in the laboratory. Work is ongoing to validate the remaining connections to the existing LHCb trigger infrastructure.

2.8 Online system

Several software upgrades to the online system were performed, namely the upgrade of the operating system from SLC6 to CentOS7 on all Linux machines, especially the HLT farm, and the upgrade of the control system infrastructure (SCADA system) from WinCCOA 3.11 to 3.15. Both upgrades went very smoothly and no adverse effects were observed.

On the hardware side, two rack rows of the HLT farm data network were upgraded to 10 GbEthernet. This was done to liberate GbEthernet line cards in the main DAQ routers, as the product used will run out of warranty towards the end of 2017. This action should guarantee safe operation for the remainder of Run 2, until the end 2018. A similar operation will be performed on the main control router, replacing 48-port linecards with 90-port cards.

In the area of application software, streamlining and optimisation of the code was performed, as well as bug fixes.

During most of the EYETS shutdown, Monte-Carlo production jobs were running on the HLT farm. On average, more than 30000 jobs were running concurrently.

3 Operations

In 2016, LHCb recorded a total integrated luminosity of $1.7\,\mathrm{fb}^{-1}$ with proton-proton collisions at a centre-of-mass energy of 13 TeV with a global efficiency of almost 90%.

The last few weeks of the year were dedicated to the proton-ion collisions. LHCb collected a total integrated luminosity of $\sim 12.5\,\mathrm{nb}^{-1}$ with proton-Pb collisions and $\sim 17.5\,\mathrm{nb}^{-1}$ with Pb-proton collisions, both at centre-of-mass energy of $\sqrt{s_{NN}} = 8\,\mathrm{TeV}$, with an efficiency of about 95%. One fill for each beam configuration was dedicated to the van der Meer scan for the evaluation of the absolute luminosity.

LHCb also collected an integrated luminosity of $\sim 0.5\,\mathrm{nb}^{-1}$ with proton-Pb collisions at centre-of-mass energy of $\sqrt{s_{NN}} = 5\,\mathrm{TeV}$. This sample, when added up to that collected in 2013, brings the total integrated luminosity in this configuration to $\sim 1.6\,\mathrm{nb}^{-1}$.

The SMOG system was used to inject helium into the VELO detector region, to act as a fixed target for the proton beam. In this configuration, the experiment took data with a proton beam energy of 4 TeV. The real-time calibration and alignment and Turbo-stream processing were successfully used for the first time during the heavy-ion operation.

Figure 7 summarises the delivered and recorded luminosity and the LHCb data collection efficiency for both the proton-proton and proton-ion collisions.

During the EYETS, several activities were carried out to further optimise and automate the data taking. They are described in detail below.

3.1 Trigger

Online-farm disk buffers with a capacity of about 10 PB are used to store the output data of the first stage of the software trigger (HLT1). This allows for real-time

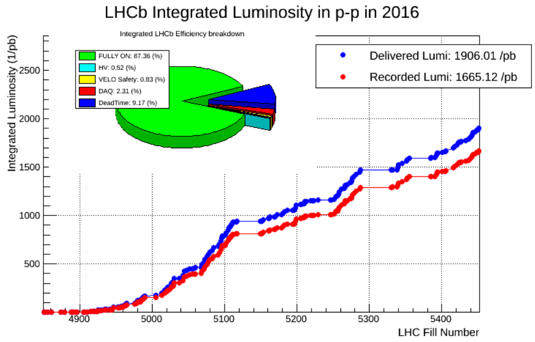

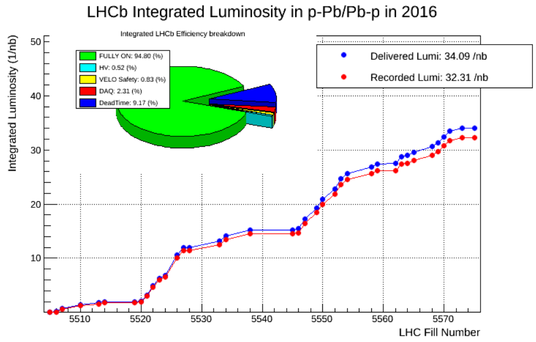

Figure 7: Delivered and recorded integrated luminosity for the 2016 proton-protons runs (left) and proton-ions runs (right), and corresponding LHCb efficiency.

alignment and calibration to be performed before the asynchronous running of the second stage of the software trigger (HLT2), with analysis-quality reconstruction. Such a strategy removes the need for further reprocessing and optimises the usage of computing resources. In 2016, the disk buffers were continuously monitored to avoid the risk of overfilling them. Two sets of HLT1 thresholds were used: a tight threshold with an output rate of 80 kHz, applied during the exceptional conditions of the LHC in June, when the machine availability was above 70%, and a loose threshold with an output rate of about 110 kHz, based on the assumption of a 40% average LHC availability. About 30% of the collected data, corresponding to a total integrated luminosity of $500\,\mathrm{pb}^{-1}$, were taken with the tight trigger configuration.

In 2017, toy models will be used to evaluate the likely evolution of the disk occupancy for the entire year. The models assume a flat LHC availability for each two-week period, uniformly distributed between 15% and 85%. A threshold change will be applied if the end-of-year projection indicates that more than 80% of the disk buffer will be filled. It is again foreseen to use two sets of HLT1 thresholds: a loose one with an output rate of 80 kHz and a tight one with an output rate of 105 kHz. An illustration of the possible evolution of the farm disk usage in 2017, from an ensemble of toy models, is shown in Fig. 8.

At the restart of the data taking, the loose HLT1 threshold will be applied and the disk occupancy projection will be evaluated assuming a 65% LHC availability. A possible change to the tight threshold will be considered only when projections indicate the risk of overfilling the buffers. A trigger configuration flag will be associated with the two HLT1 selections to simplify data selection at the analysis level.

The L0 thresholds for all physics channels will be optimised following last year's procedure. However, an additional selection will be applied to reduce the effect of hits from tracks from previous bunch crossings (spill-over hits). As discussed in Sec. 2.3, spill-over is particularly relevant for the OT, where it produces a considerable increase in the straw occupancy. Events severely affected by spillover can be rejected by applying a selection on the total transverse energy collected

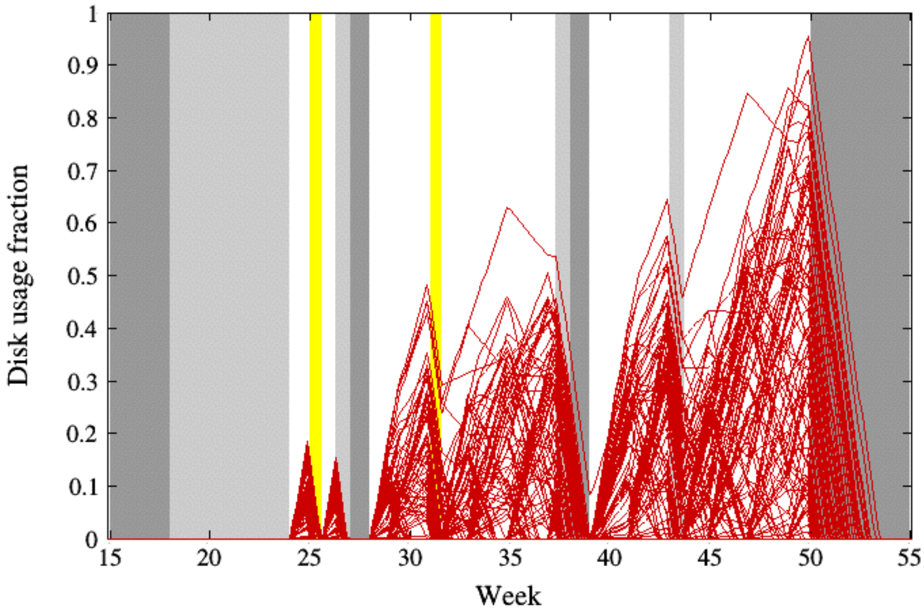

Figure 8: Predicted evolution of the farm disk usage in 2017 based on toy models with the assumption of a flat LHC availability for each 2-week period, uniformly distributed between 15% and 85%.

by the calorimeters in the previous event. This procedure has been studied using dedicated data collected at the end of 2016 with both magnet polarities. This additional selection results in unchanged rates for both L0 and HLT1; moreover, the HLT processing speed is increased by ∼2% in the HLT1 step and by almost 5% in the HLT2 step. Different sets of L0 thresholds will be provided before the start of the data taking based on an optimisation that depends on the LHC filling scheme.

3.2 Reconstruction

Several algorithms have been optimised, including the T-station track reconstruction and the calorimeter and RICH PID, resulting in a globally faster reconstruction. In particular, work performed in the context of the LHCb upgrade has allowed the speed of the RICH reconstruction to be improved by $\mathcal{O}(30\%)$. As a result, the RICH PID information available in HLT2 can also be extended to downstream tracks (these are tracks produced by particles decaying after the VELO), greatly benefiting all physics analyses based on long lived-particles.

3.3 Turbo and Calibration streams

The Calibration stream provides pure data samples of pions, kaons, protons, muons and electrons that can be used to determine PID and tracking efficiencies in a datadriven method. Events sent to the Calibration stream contain the stored trigger candidates in addition to the raw sub-detector data. During the EYETS, samples of neutral particles (both photons and π^0) as well as particle samples originating from downstream tracks have also been included in the stream.

The Turbo stream is a compact event record written directly from the trigger and available for physics analysis bypassing the offline reconstruction. In 2016 the possibility was implemented to save the entire trigger-reconstructed event. This led to an increase of the Turbo-output bandwidth by more than a factor of three and to a significant increase of the stream size. A considerable effort is being invested to reduce the resources required by the Turbo, without limiting the physics analyses which make use of it. Two new concepts have been introduced: 1) a selective saving of raw banks defined by the specific physics analyses and 2) a selective saving of additional objects in the event. This implementation is well advanced and will be ready for the restart of the data taking.

3.4 Real-time alignment and calibration

The real-time alignment and calibration procedure ran smoothly in 2016, with an automatic update of the VELO and tracker (TT, IT and OT) alignment constants. Figure 9 shows the variation as a function of time for some of the VELO and IT alignment constants. Typically, an update of the VELO and of the tracker parameters is expected often, but not for every fill. The alignment procedure for the muon stations was run at the beginning of each fill but only as a monitoring tool, as the alignment is not expected to vary except in case of hardware interventions. The RICH mirror alignment was also monitored and no significant variations were observed.

In 2016, the electromagnetic calorimeter was calibrated on a fill-by-fill basis using a LED system that automatically evaluated the HV settings needed to compensate for detector ageing effects. The absolute calibration was obtained during technical stops by performing dedicated fits to the invariant mass distribution of $\pi^0 \to \gamma\gamma$ decays for every cell in the ECAL. During the EYETS, the π^0 calibration was completely reviewed and work is progressing towards an automatic calibration to be performed every few weeks on the online farm. As discussed in Sec. 2.5, a new software package is being developed that shows speed improvements by an order of magnitude. It is expected that its implementation will be ready for the restart of data taking.

In previous years, the alignment and calibration constants for those sub-systems that only require one or two updates per year had not been migrated to the Online DB. During the EYETS, it was decided to move all alignment and calibration constants to the online DB. This required an update of several scripts as well as thorough testing of the consistency of the constants used in the online and offline environments. The transition is currently being completed.

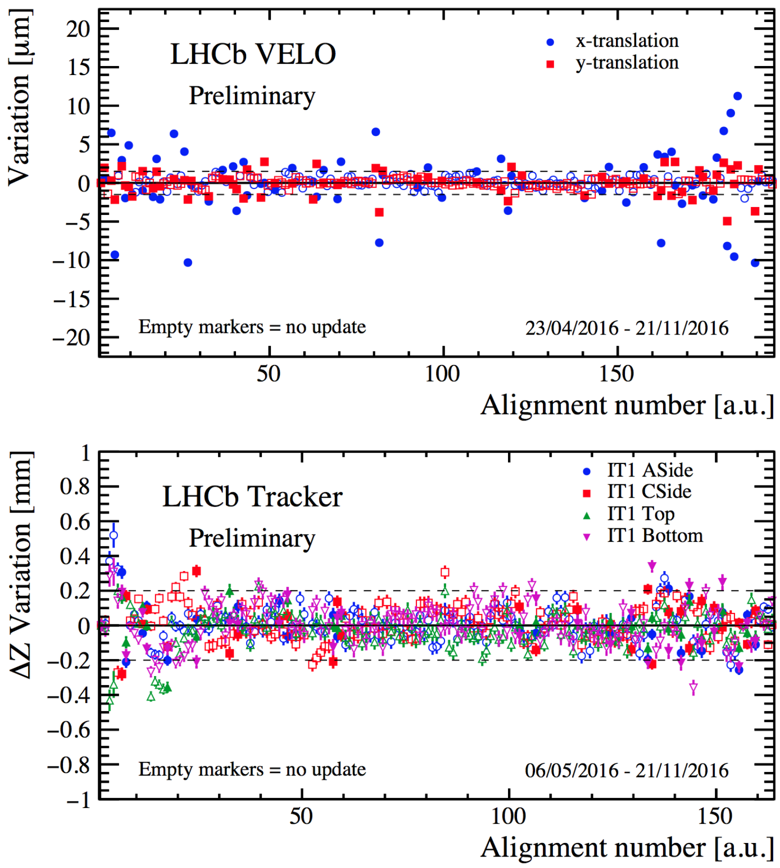

Figure 9: Variation in time for some of the VELO (top) and IT boxes (bottom) alignment constants. Each point indicates the difference from the previous set of constants while the dashed lines indicate the threshold required to update the constants.

3.5 Data Quality (DQ)

The DQ monitoring for Run 2 has been updated to a web-based framework, which allowed most DQ shifts to be organised remotely. More than 98% of the data were flagged as good for physics. During the EYETS, real-time monitoring was also migrated to the new web-based framework and work is ongoing to commission it for the 2017 data taking.

3.6 Computing

The computing usage for 2016 [6] and the computing resources needed by LHCb in 2018, with a preview of the 2019 requests [7], based on the latest measurements of the LHCb computing model parameters and latest updates of the LHC running plans, are discussed in detail in separate documents.

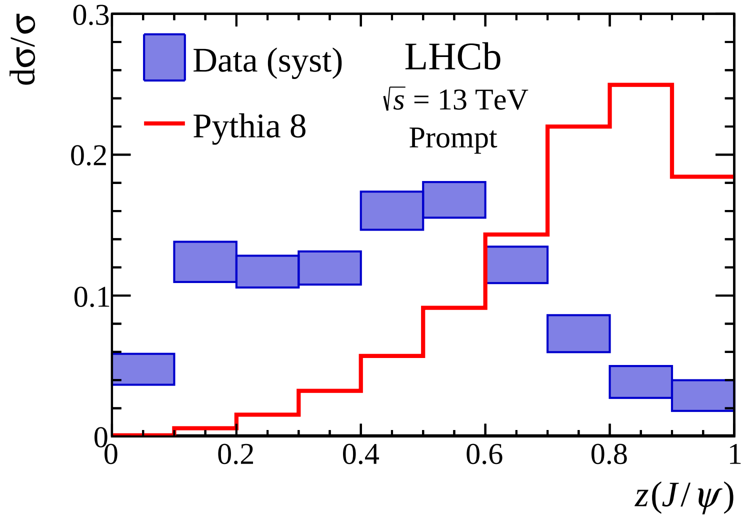

Figure 10: Measured normalized $z(J/\psi)$ distributions for J/ψ mesons produced in b-hadron decays, compared to predictions obtained from Pythia 8 [8].

4 Physics results

Since the last RRB in October 2016, LHCb submitted 29 new publications, for a total of 370 papers at the time of writing. Ten further publications are being processed by the Editorial Board and are close to submission. In the following, some results in the sectors of heavy flavour production and spectroscopy, fixed-target physics, rare decays and *CP* violation are highlighted.

4.1 Heavy flavour production and spectroscopy

The production of J/ψ mesons in jets at a centre-of-mass energy of 13 TeV was studied [8]. The fraction of the jet transverse momentum carried by the J/ψ meson, $z(J/\psi) = p_{\mathrm{T}}(J/\psi)/p_{\mathrm{T}}(\text{jet})$, is measured using jets with $p_{\mathrm{T}}(\text{jet}) > 20\,\text{GeV}$ in the pseudorapidity range $2.5 < \eta(\text{jet}) < 4.0$. The observed $z(J/\psi)$ distribution for J/ψ mesons produced in b-hadron decays is consistent with expectations. However, the results for prompt J/ψ production do not agree with predictions based on fixed-order non-relativistic QCD obtained from Pythia 8, as shown in Fig. 10. This is the first measurement of the p_{T} fraction carried by prompt J/ψ mesons in jets at any experiment.

In the sector of spectroscopy, an amplitude analysis of the decay $\Lambda_b^0 \to D^0 p\pi^-$ was performed in the part of the phase space containing resonances in the $D^0 p$ channel [9]. The spectrum of excited Λ_c^+ states that decay into $D^0 p$ was studied, measuring masses, widths and quantum numbers of the $\Lambda_c(2880)^+$ and $\Lambda_c(2940)^+$ resonances. The constraints on spin and parity of the $\Lambda_c(2940)^+$ state were obtained for the first time. A near-threshold enhancement in the $D^0 p$ amplitude was investigated and found to be consistent with a new resonance, denoted by

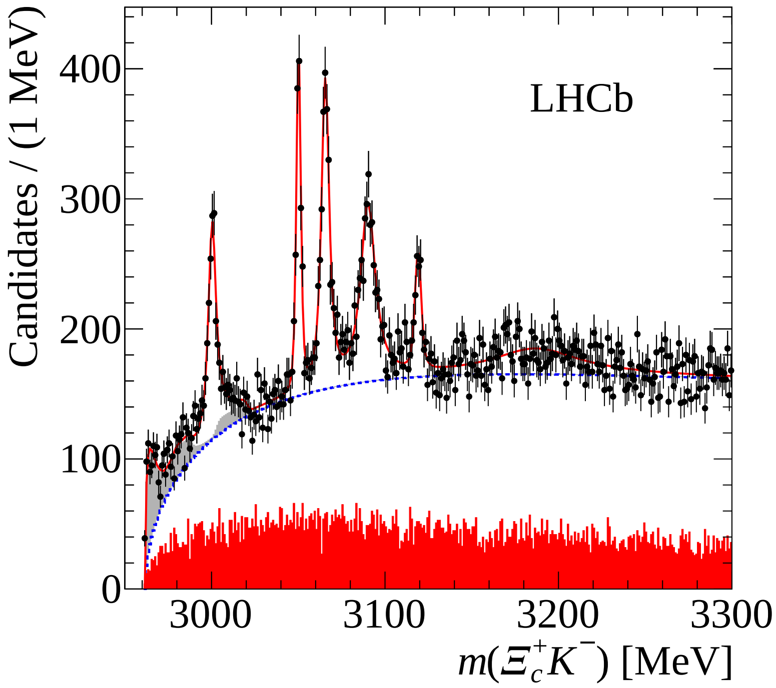

Figure 11: Reconstructed invariant mass $m(\Xi_c^+ K^-)$. The solid (red) curve shows the result of the fit, and the dashed (blue) line indicates the fitted background. The shaded (red) histogram shows the corresponding mass spectrum from the Ξ_c^+ sidebands and the shaded (light gray) distributions indicate the feed-down from partially reconstructed Ω_c^0 resonances [1].

$\Lambda_c(2860)^+$, of spin $3/2$ and positive parity. A search for resonances in the $\Xi_c^+ K^-$ mass spectrum was performed [1], with the Ξ_c^+ decaying to the $pK^-\pi^+$ final state. Five new, narrow excited Ω_c^0 states were observed, as shown in Fig. 11.

4.2 Fixed-target physics

The first LHCb analysis of heavy flavour production in fixed-target mode was shown as a preliminary result at Quark Matter 2017 [2]. The J/ψ and D^0 production processes were studied in 6.5 TeV proton-beam-induced reactions on an argon gaseous target. About 500 $J/\psi \to \mu^+\mu^-$ and 6500 $D^0 \to K^-\pi^+$ decays were reconstructed. Their yields were studied as a function of transverse momentum, rapidity, Bjorken-x and Feynman-x. No strong dependence of the J/ψ / D^0 cross-section ratio on rapidity was observed, as shown in Fig. 12.

More recently, another fixed-target preliminary result was presented at the Rencontres de Moriond 2017. The antiproton production cross-section in collisions of a 6.5 TeV LHC proton beam on helium at rest was measured using the SMOG internal gas target [3]. This is the first direct measurement of antimatter production in pHe collisions, and has important implications for the interpreta-

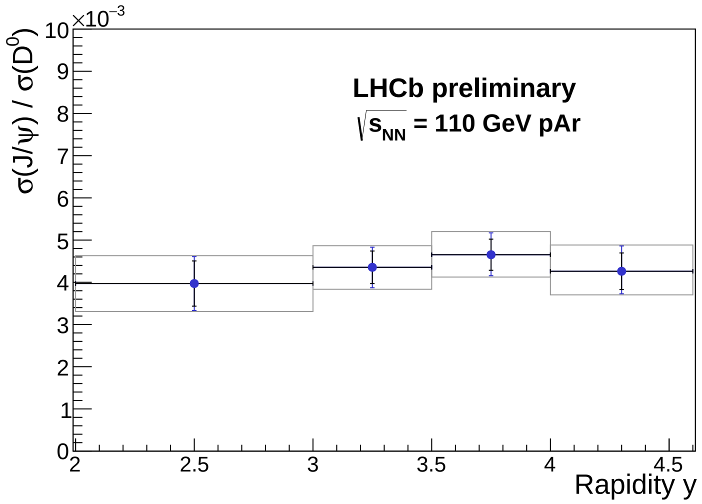

Figure 12: J/ψ to D^0 cross-section ratio as a function of rapidity [2].

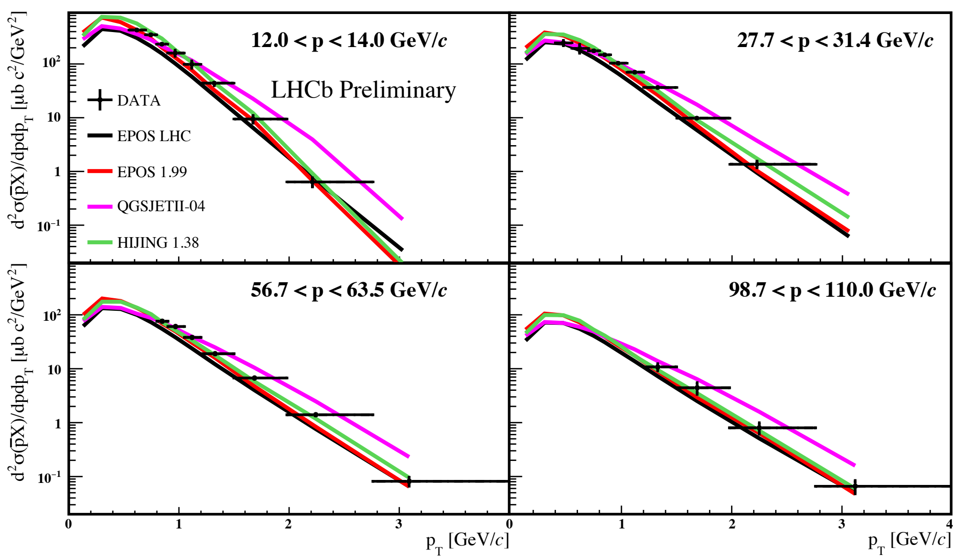

Figure 13: Antiproton production cross-section as a function of transverse momentum in four different bins of momentum [3]. The predictions of various event generators are superimposed.

tion of recent results from the PAMELA and AMS-02 experiments, measuring the antiproton component in cosmic rays in space. The antiproton production cross-section as a function of transverse momentum in four different bins of momentum is shown in Fig. 13. As it is apparent, there is a large spread amongst the various models, hence the LHCb reasults provide a strong constraint.

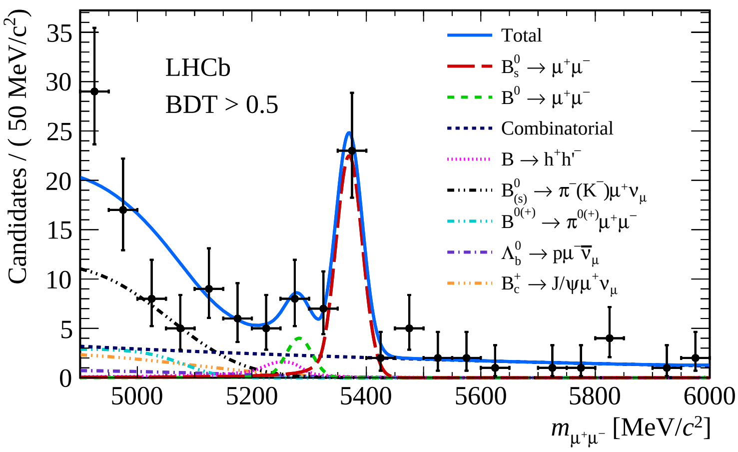

Figure 14: Mass distribution of $B^0_{(s)} \to \mu^+\mu^-$ candidates selected requiring good purity [4].

4.3 Rare decays

A new search for the rare decays $B^0_s \to \mu^+\mu^-$ and $B^0 \to \mu^+\mu^-$ was performed by LHCb using data corresponding to a total integrated luminosity of $4.4\,\text{fb}^{-1}$ [4]. The $B^0_s \to \mu^+\mu^-$ signal was measured with a significance of 7.8 standard deviations, representing the first observation of this decay from a single experiment. The branching fraction was measured to be $(3.0 \pm 0.6\,^{+0.3}_{-0.2}) \times 10^{-9}$, where the first uncertainty is statistical and the second systematic. Furthermore, the first measurement of the $B^0_s \to \mu^+\mu^-$ effective lifetime was reported to be $2.04 \pm 0.44 \pm 0.05\,\text{ps}$. No significant excess of $B^0 \to \mu^+\mu^-$ decays was found and a 95% confidence level upper limit, 3.4×10^{-10}, was determined. All results are in agreement with the Standard Model expectations. The mass distribution of candidates selected requiring good purity is shown in Fig. 14.

A similar search for $B^0_{(s)} \to \tau^+\tau^-$ decays was performed using the full Run 1 data sample of $3\,\text{fb}^{-1}$. The τ leptons were reconstructed through the decay $\tau^- \to \pi^-\pi^+\pi^-\nu_\tau$. Assuming no contribution from $B^0 \to \tau^+\tau^-$ decays, an upper limit was set on the branching fraction of the $B^0_s \to \tau^+\tau^-$ decay at 6.8×10^{-3} with 95% confidence level. If instead no contribution from $B^0_s \to \tau^+\tau^-$ decays is assumed, the limit for $B^0 \to \tau^+\tau^-$ is $< 2.1 \times 10^{-3}$ with 95% confidence level. These results provide the first experimental limit on $\mathcal{B}(B^0_s \to \tau^+\tau^-)$ and the world's best limit on $\mathcal{B}(B^0 \to \tau^+\tau^-)$.

4.4 *CP* violation

Measurements of the time-dependent *CP*-violating observables in $B^0_s \to D_s^{\mp}K^{\pm}$ decays were performed using the full Run 1 data set [10]. Such observables were used together with a recent measurement of the B^0_s mixing phase $-2\beta_s$ to obtain a measurement of the CKM angle γ. The resulting confidence interval for

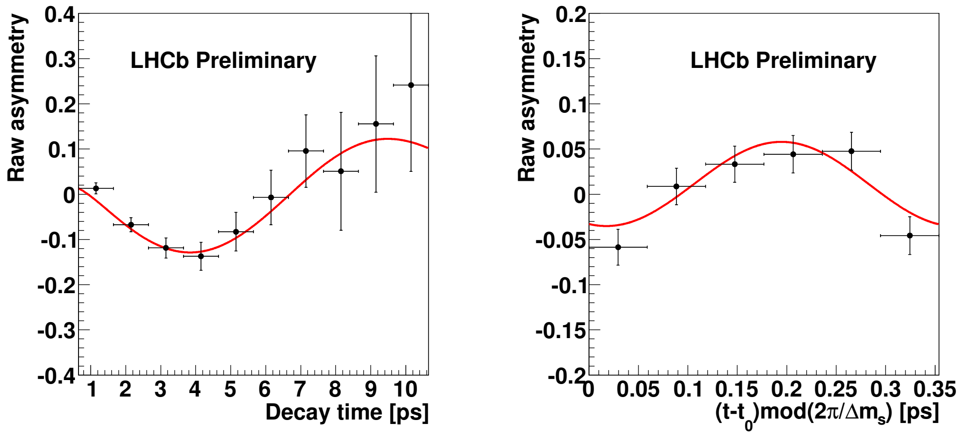

Figure 15: Time-dependent asymmetries for (left) $B^0 \to \pi^+\pi^-$ and (right) $B_s^0 \to K^+K^-$ decays from candidates lying in the signal invariant mass regions [11]. The offset $t_0 = 0.6\,\text{ps}$ corresponds to the selection requirement on the minimum decay time.

γ is $(127^{+17}_{-22})^\circ$ at 68% confidence level, corresponding to a 3.6 σ evidence for *CP* violation in $B_s^0 \to D_s^\mp K^\pm$.

Another relevant set of time-dependent measurements of *CP* violation in the decay and in the interference between mixing and decay were performed in $B^0 \to \pi^+\pi^-$ and $B_s^0 \to K^+K^-$ decays using the full Run 1 data set [11]. For this preliminary result, flavour tagging was performed using only a subset of the current available taggers. The measurements are in good agreement with previous measurements by BaBar and Belle. The measurement of *CP* violation in the interference between mixing and decay for the $B^0 \to \pi^+\pi^-$ mode is the most precise from a single experiment to date. No other experiment has ever measured *CP* violation in $B_s^0 \to K^+K^-$; a strong evidence of 4.7 σ is found in this analysis. The time-dependent asymmetries for the $B^0 \to \pi^+\pi^-$ and $B_s^0 \to K^+K^-$ decay modes are shown in Fig. 15. Further improvements in precision are expected with the inclusion of same-side flavour tagging information in the final measurement.

5 Financial issues

The status of the accounts is healthy and no cash flow problems are foreseen. The expenditure on the 2016 M&O Cat. A budget followed forecasts well. As expected, a small overspending is registered, due to late bills from 2015 and to the anticipated acquisition of a new farm slice (CERN-RRB-2016-113). As proposed in CERN-2016-RRB-114 and accepted by the RRB, the 2015-year surplus has been used to offset the overspending from this year.

6 Collaboration matters

In December, Giovanni Passaleva (INFN Firenze) was elected as the next LHCb Spokesperson. He will begin his mandate in July 2017 and serve for a period of three years. In March, Los Alamos National Laboratory, USA, was elected as an associate member of the collaboration.

References

[1] LHCb collaboration, R. Aaij *et al.*, *upcoming analysis*, LHCb-PAPER-2017-002, in preparation.

[2] LHCb collaboration, *Measurement of J/ψ and D^0 production in pAr collisions at $\sqrt{s_{NN}} = 110\ GeV$*, LHCb-CONF-2017-001.

[3] LHCb collaboration, *Measurement of antiproton production in pHe collisions at $\sqrt{s_{NN}} = 110\ GeV$*, LHCb-CONF-2017-002.

[4] LHCb collaboration, R. Aaij *et al.*, *Measurement of the $B^0_s \to \mu^+\mu^-$ branching fraction and effective lifetime and earch for $B^0 \to \mu^+\mu^-$ decays*, LHCb-PAPER-2017-001, in preparation.

[5] LHCb collaboration, *Status of the LHCb upgrade*, CERN-RRB-2017-036.

[6] C. Bozzi, *LHCb Computing Resource usage in 2016 (II)*, Tech. Rep. LHCb-PUB-2017-010. CERN-LHCb-PUB-2017-010, CERN, Geneva, Feb, 2017.

[7] C. Bozzi, *LHCb Computing Resources: 2018 requests and preview of 2019 requests*, Tech. Rep. LHCb-PUB-2017-009. CERN-LHCb-PUB-2017-009, CERN, Geneva, Feb, 2017.

[8] LHCb collaboration, R. Aaij *et al.*, *Study of J/ψ production in jets*, `arXiv:1701.05116`, submitted to Phys. Rev. Lett.

[9] LHCb collaboration, R. Aaij *et al.*, *Study of the D^0p amplitude in $\Lambda^0_b \to D^0p\pi^-$ decays*, LHCb-PAPER-2016-061, in preparation.

[10] LHCb collaboration, *Measurement of CP asymmetry in $B^0_s \to D^{\mp}_s K^{\pm}$ decays*, LHCb-CONF-2016-015.

[11] LHCb collaboration, *Measurement of time-dependent CP violating asymmetries in $B^0 \to \pi^+\pi^-$ and $B^0_s \to K^+K^-$ decays at LHCb*, LHCb-CONF-2016-018.